

removal would result in the creation of smoothly polished surfaces. Here, film removal is envisaged to happen when the oxide films are only a few tens of nanometres thick. Essentially, this process is identical to that conceived for Type I corrosion-wear that affects uncoated and certain coated stainless steels when immersed in aqueous saline solutions and subjected to sliding contact with an inert material (Dearnley & Aldrich-Smith, 2004 – see **Fig. 6.44** in **Chapter 6**). In the case of piston ring/cylinder liner contacts, the ability to resist polishing due to CW is a reflection of the adhesive strength of the oxide film to its parent coating. One possible explanation for some of the results shown in **Fig. 8.20b** is that Cr-N-O films formed above CrN coatings are more tenaciously bonded than Cr-B-O films formed above Cr-33B and Cr-26B coatings. Similarly, W-B-O films are weakly attached to W-25B coatings. Notably, the Cr-33B coating – although harder than the Cr-26B coating (**Fig. 8.20a**) – was worn to a greater extent (**Fig. 8.20b**). This suggests that a higher B content in a Cr-B-O film results in a more weakly attached oxide film, resulting in a greater surface material loss.

### 8.3 Surface Engineering of Valve Lifters (Cam-Followers)

#### 8.3.1 Background

Valve lifter (cam-follower) and cam shaft materials have *not* received very much change in the past thirty years. The review of Becker (2004) indicates no changes in the principal materials used for these devices when compared to those highlighted in publications during the 1980s (Eyre & Crawley, 1980; Eyre, 1984). The summary given in **Table 8.3** is still relevant at the time of writing (circa 2015); this shows a high reliance on cast irons and steels for valve lifters and cams. Here, surface engineering is required to realise a combination of high fatigue endurance, fatigue strength, rolling contact fatigue (RCF) pitting resistance, micro-abrasion wear and scuffing (material transfer) resistance. Scuffing is minimised by the phosphating (with manganese phosphate) of steel or cast iron valve lifters or by using micro-cracked Cr electroplating (similar to that shown in **Fig. 8.4a**). The latter procedures enable oil retention and spreading, which greatly aid boundary lubrication. Formulated oils containing anti-wear additives, like ZDDP (Bec et al, 1999; Barnes et al, 2001; Spikes, 2004; de Barros Bouchet et al, 2005), although widely used to aid an anti-scuffing character, can also initiate premature rolling contact fatigue pitting (Eyre & Crawley, 1980). Adverse pinholing of DLC coatings (presently being introduced for valve lifter applications) may also be triggered by oil additives (**Section 8.3.3**).

Cams are not generally coated but are frequently hardened by induction or flame hardening (to form a martensitic case) or may be nitrided (refer to **Chapters 3 & 5**). In these situations, the aim is to increase RCF pitting resistance and enhance rotation bending fatigue endurance and strength. When micro-abrasion wear resistance (MAWR) is a concern (**Table 8.3**), as in some diesel engine applications where abrasive soot particles may ingress the lubricating oil, the cam ‘nose’ is subjected to rapid cooling (‘chill casting’) during its manufacture; this forms a durable, hard

Table 8.3 Common camshaft and valve lifter (cam follower) materials developed in the 1980s which remain in use today (circa 2015). Based on data and comments of Eyre & Crawley, 1980.

Camshaft materials	Purpose of treatment	Valve lifter materials	Purpose of treatment
Chilled cast iron (cam nose)	‡MAWR	Chilled cast iron	‡MAWR, scuffing resistance
Induction-hardened SG-iron	‡MAWR; scuffing resistance, *RCF pitting reduction, increased ¥RBFE	Induction-hardened SG-iron	‡MAWR, scuffing resistance, *RCF pitting reduction
Induction-hardened alloy cast iron	‡MAWR; scuffing resistance, *RCF pitting reduction, increased ¥RBFE		
Induction-hardened pearlitic malleable cast iron	‡MAWR; *RCF pitting reduction, scuffing resistance, increased ¥RBFE	Hard (micro-cracked) chromium-plated steels or cast iron	‡MAWR, scuffing resistance and oil spreading
Forged and carburised 0.1%C steel	‡MAWR; *RCF pitting reduction, scuffing resistance, increased ¥RBFE.	Carbonitrided 1.5% Mn-Mo steel	‡MAWR, scuffing resistance, *RCF pitting reduction
Forged and induction-hardened 0.3%C steel	‡MAWR; *RCF pitting reduction, scuffing resistance, increased ¥RBFE	Mn phosphated [(Mn <sub>3</sub> (PO <sub>4</sub> ) <sub>2</sub> )] steel	Scuffing resistance, oil spreading and running-in assistance
		Gas nitrided steel**	Scuffing and *RCF pitting reduction

‡ MAWR= micro-abrasion wear resistance  
\* RCF=rolling contact fatigue  
¥ RBFE=rotation-bending fatigue endurance and strength  
\*\* Supersedes the original salt bath nitriding (Tufftriding) method quoted by Eyre & Crawley, 1980.

(Hv~1200 kg/mm<sup>2</sup>) surface zone of cementite (Fe<sub>3</sub>C). However, its brittle nature has the potential to reduce rotation bending fatigue endurance and strength.

A major factor in materials selection for cams and valve lifters remains production costs. These are lowest of all for castings in cast iron (Birch, 2009), despite valiant efforts by enterprising manufacturers to utilise alternative near-net-shape production routes like powder technology (for modular steel cams) – Becker (2004). Other innovations to develop durable silicon nitride ceramic valve lifters, despite showing promise (Kano & Tanimoto, 1991a,b), were not subsequently exploited for mass production motor vehicle use due to their relatively high production and raw material costs compared to those of steels and cast irons. Nowadays there are other concerns. The use of phosphating (Fig. 5.13) and electroplating (Fig. 4.18) technologies (specified for valve lifters – Table 8.3) is under legislative threat due to perceived negative environmental impact concerns. This has led to efforts to replace these processes with environmentally friendly techniques like PVD or PACVD. The latter are used for production of DLC (diamond-like carbon), CrN and Cr<sub>2</sub>

N (chromium 2 nitride) coatings. The potential of the latter for use in oil-lubricated operating environments, relevant to the valve lifter/cam-follower situations, is now discussed in some detail.

The operational range of lubrication regimes for a cam and cam lifter system is narrower than that for piston ring/cylinder liner (**Fig. 8.2**), and typical friction levels (Taylor, 1991) are very much lower ( $\mu < 0.01$ ) due to the opposing surfaces experiencing a range of contact conditions from pure sliding, to a mix of sliding and rolling, to pure rolling. The increasing use of lower-viscosity oils brought about by changing from mineral or semi-synthetic oils to fully synthetic oils (to attain better fuel economy) – combined with changes in oil additive packages to reduce unwanted negative environmental impact element emissions (like Zn and P) – has brought about more demanding operating conditions for the cam/valve lifter system. Such changes have caused a higher probability of inter-material contact, which has led to adverse component wear. Accordingly, there has been significant interest in evaluating the prospect of increasing component life through the application of surface treatments to cams or valve lifter surfaces, including efforts to develop diamond-like carbon coatings (Ford Motor Company, 1993a,b; Sjöström & Wikström, 2001), which has culminated in at least one Japanese manufacturer applying such coatings to the valve lifter components of one mass-production engine.

### 8.3.2 Experimental Aspects

The assessment of the suitability of coating materials for cam/valve lifter systems is both time consuming and costly to carry out in fully instrumented ‘fired’ engine test cells (with full (direct plus indirect) costs being ~\$30,000 per test) or even using electrically ‘motored’ cam shaft/cylinder head systems, so a cheaper alternative is required. Simple-configuration oil-lubricated pin-on-plate or pin-on-disc labs tests, although used by some (Austin et al, 2012), are too basic to obtain meaningful test results and are carried out under non-realistic time frames. To the knowledge of the author, there have been several large-scale development projects where successful pin-on-plate results (obtained on coated test-pieces) have not translated into positive results when scaled up to more-advanced engine test-cell environments. The most likely reason for this difficulty is that contacting stresses in internal combustion engine cam/valve lifters are not constant – they are cyclic. Here, surface contacts are subjected to high-speed ( $> 2$  m/sec), high-frequency ( $\sim 50\text{Hz} = 3000\text{revs/min}$ ) stressing where the maximum Hertz contact stress ranges ( $P_{\text{max}}$  – see **Chapter 2, Section 2.4**) from  $\sim 200$  to  $\sim 1500\text{MPa}$  (0.2 to 1.5GPa), depending upon the engine specification. To overcome this difficulty, an alternative experimental approach is required to evaluate would-be prototype surface engineered cam follower/valve lifter components. One successful method is to use a thrust bearing experimental set-up (Gold & Loos, 2002; Yonekura et al, 2005; Dearnley et al, 2014), **Fig. 8.23** and **Fig. 8.24**. This approach allows very high numbers of stress cycles to be accumulated in comparatively ‘short’ test times. In the set-up shown in **Fig. 8.23** three coated test rollers (retained within a plastic bearing cage) are rotated by the action of an

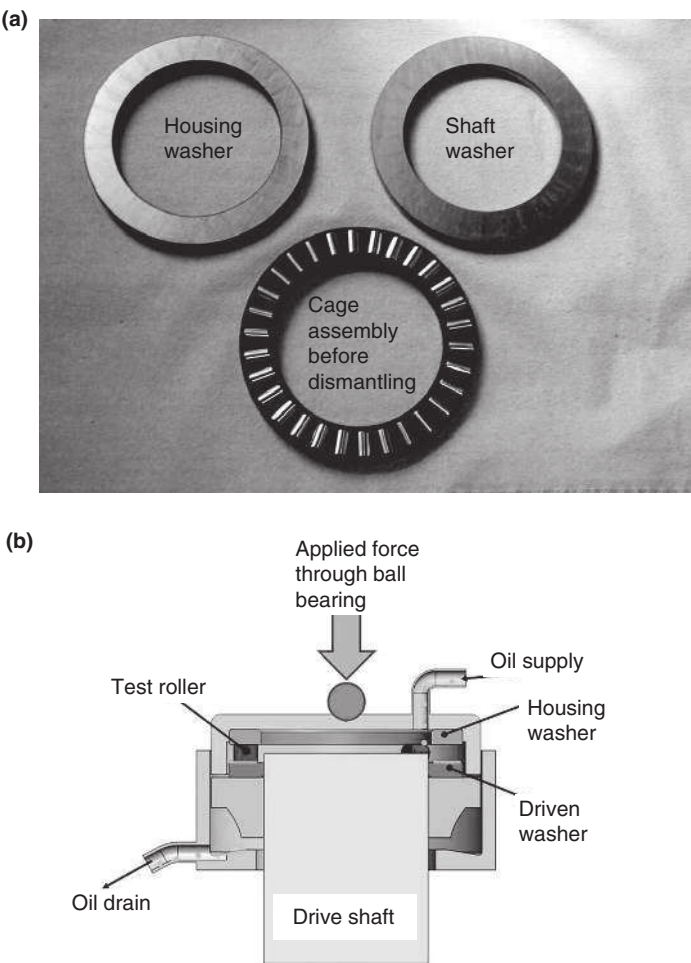


Figure 8.23 Details of thrust bearing test components: (a) disassembled thrust bearing showing roller bearings (only three rollers actually used per test), housing bearing ring/washer and driven shaft ring/washer; (b) schematic section through the test head/housing.

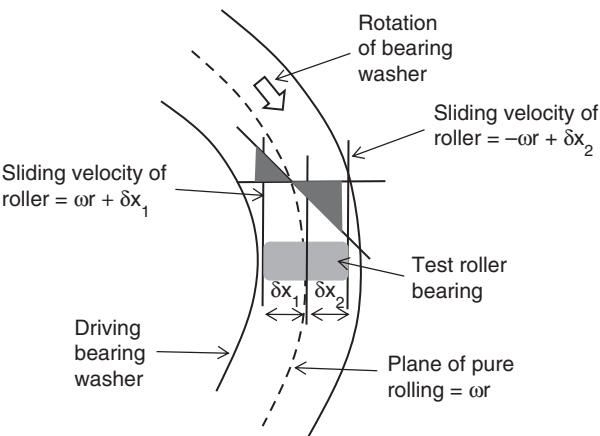


Figure 8.24 Kinematics of the rolling and sliding components of a cylindrical roller bearing in contact with a driving washer bearing contained in a thrust bearing test rig.

uncoated shaft washer, ‘driven’ at 1450 rpm, against an uncoated stationary washer, whilst the entire assembly is flooded with oil lubricant. The thrust bearing assembly causes a combination of sliding and rolling action to be transferred to each test roller, mimicking the cam/valve lifter stress cycle behaviour. In two reported experimental works (Yonekura et al, 2005; Dearnley et al, 2014), the rotation of each coated test roller was such that its surface was subjected to rolling and sliding velocities of ~2.5m/s and 0.25m/s respectively, realised by 20 rotations of each roller as it traversed the bearing circumferential path. By using two thrust bearing machines, a high number of used test-pieces were generated. In all cases, a range of maximum Hertzian contact pressures from 0.5 to 1.5GPa was deployed. To permit these extreme conditions, very high strength through hardened, martensitic, bearing steel (100Cr6) substrates were selected, with a Vickers microhardness (Hv) of 760kg/mm<sup>2</sup> (~7.6GPa), which equated to an approximate uniaxial yield strength of 2.5GPa (Yonekura et al, 2005). This procedure allowed many thousands of stress cycles to be applied to uncoated and coated test-pieces over a relatively short period of testing (a few days).

8.3.3 Some Experimental Results

This section is largely based on the experimental results obtained by Yonekura et al (2005) and Dearnley et al (2014). Here, mineral oils, with and without specific oil additives, were deployed as a lubricant. The former is referred herein as ‘base oil’, whilst the latter is termed ‘formulated oil’; this conformed to the SAE 10W-40 specification. Whilst several PVD/PACVD coating materials (all applied to through-hardened 100Cr6 substrates) were evaluated, only three of these are reconsidered here (**Table 8.4**): W-doped H:DLC (a hydrogenated DLC), ta-C DLC [a non-doped, non-hydrogenated, tetragonal (ta) carbon-rich DLC] and PVD-Cr<sub>2</sub>N. The DLC coatings were ~1 to 2µm thick, whilst the Cr<sub>2</sub>N coatings were ~2µm thick.

Scuffing and Galling (Metal Transfer)

Although in principle possible, this mechanism was not observed for uncoated or coated rollers or their corresponding washers. It would appear that martensitic steel

Table 8.4 *Coating materials applied to 100Cr6 martensitic steel roller bearings for thrust bearing tests. Reported by Yonekura et al (2005) and Dearnley et al (2014).*

Coating material	Hydrogenated?	Thickness (µm)	Sp3/Sp2 content	Compressive internal stress (GPa) <sup>#</sup>	Load invariant Vickers hardness <sup>*</sup> (kg/mm <sup>2</sup> ; ~GPa)
W-doped H:DLC	Yes	2.00±0.04	35/65	0.8	1524–1800 (15–18)
ta-C DLC (tetragonal carbon rich)	No	1.77±0.21	80/20	4–6	3100 (31)
Cr <sub>2</sub> N	No	2.0±0.20	N/A	Not determined	1721 (17)

<sup>\*</sup> Determined using the method devised by Vingsbo et al, 1986. Also refer to **Chapter 2, Section 2.6**.  
<sup>#</sup> Determined using the method of Stoney (1909).

(100Cr6), due to its very high shear yield strength ( $\sim 1.2\text{GPa}$ ), is too strong to be sheared (or smeared) out and transferred to the counterface material concerned, since the estimated shear stress acting on the surface was only  $\sim 5\text{MPa}$  (based on a friction coefficient of  $\sim 3.5 \times 10^{-3}$ ; see **Fig. 8.38**). This observation supports the justification for selecting martensitic steels (carburised, carbonitrided or induction-hardened steels and cast irons) – found in many internal combustion engine cams and valve lifter components (**Table 8.3**) – which have similar surface strengths.

**Micro-Abrasion Wear (MAW), Third-Body Abrasion or Polishing Wear**

Following testing (Yonekura et al, 2005; Dearnley et al, 2014), evidence of mechanical polishing due to MAW was observed on the uncoated martensitic 100Cr6 rollers and washer counterfaces (**Fig. 8.25**) as well as on the surfaces of the DLC (**Fig. 8.26**) and  $\text{Cr}_2\text{N}$  coated 100Cr6 materials. This phenomenon is presumed to be due to cutting and/or ploughing action of hard particles rubbing against the coated/uncoated washer/roller surfaces. The extent of washer micro-polishing was dependent on the coating hardness of the opposing coated rollers. In one instance, the MAW of uncoated 100Cr6 steel washers was less when tested against 100Cr6 rollers coated with W-doped H:DLC than when used against rollers coated with ta-C (tetrahedral carbon rich) DLC. This was demonstrated by the observation that the original surface grinding marks of the 100Cr6 washers (**Fig. 8.25a**) were completely removed by contact with the harder ( $\text{Hv} \sim 3000\text{kg/mm}^2$ ) ta-C DLC coating (**Fig. 8.25b**), whilst these features were still visible after testing against the less hard ( $\text{Hv} \sim 1700\text{kg/mm}^2$ ) W-doped H:DLC-coated rollers (**Fig. 8.25c**).

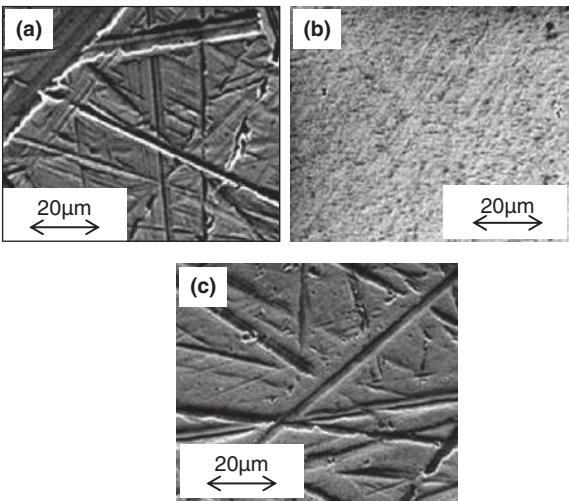


Figure 8.25 Surfaces of uncoated thrust bearing washers: (a) original; (b) after testing against ta-C DLC-coated 100Cr6 roller; (c) after testing against W-doped H:DLC-coated 100Cr6. The wear is attributed to micro-abrasion. Tests carried out in base oil for approximately the same time.

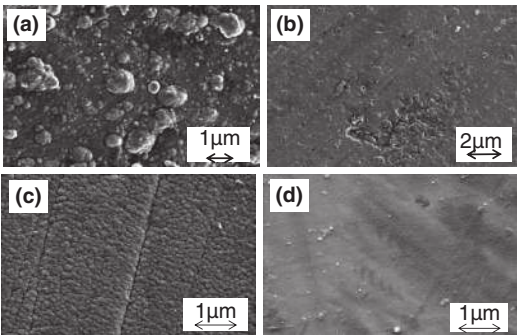


Figure 8.26 Surfaces of: (a) original; (b) smoothly worn ta-C DLC-coated 100Cr6 roller; (c) original and smoothly worn; (d) W-doped H: DLC-coated 100Cr6. The wear is attributed to micro-abrasion. Tests carried out in base oil. After Dearnley et al, 2014.

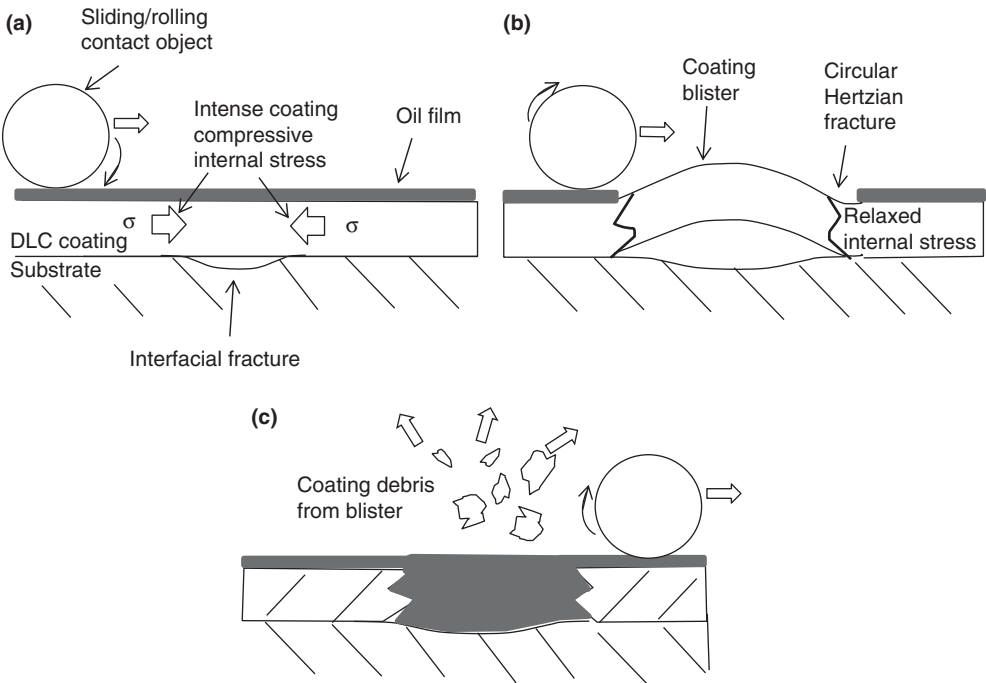


Figure 8.27 Schematic sketch showing: (a) crack initiation/growth at the DLC coating/100Cr6 steel substrate interface; (b) subsequent coating relaxation after blister formation; and (c) wear debris creation caused by blister fracture in an oil lubricated rolling/sliding contact.

Coating Delamination (Spalling) along the Coating/Substrate Interface

Whilst coating loss via delamination along the coating/substrate interface can evidently take place for some PVD-coated stainless steel piston rings (**Fig. 8.17**), the character of a nominally similar effect – created by the cyclic high-pressure contact in thrust bearing tests – was different. The latter process is initiated by local interfacial crack propagation, followed by coating blister formation. The blisters subsequently become decapitated (during contact with the counter-surface). This effect is depicted schematically in **Fig. 8.27**. Supporting evidence for the early stages of

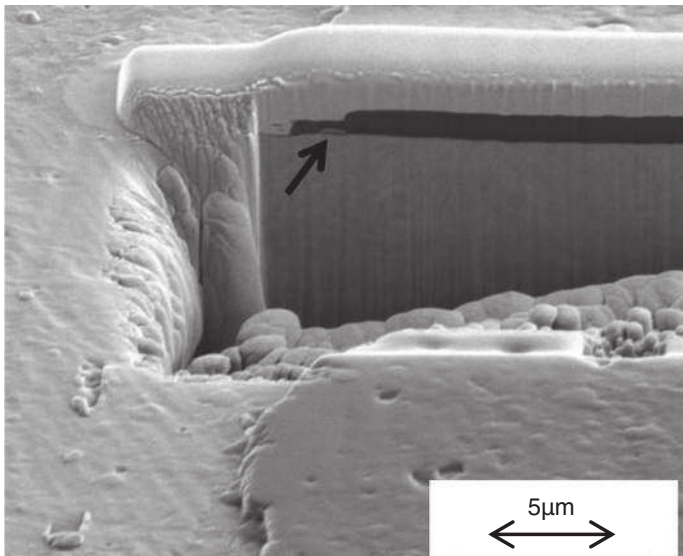


Figure 8.28 FIB section showing coating/substrate interface cracking (arrow) of a non-doped, non-hydrogenated, DLC-coated 100Cr6 adjacent to a major tear, after several million test cycles.

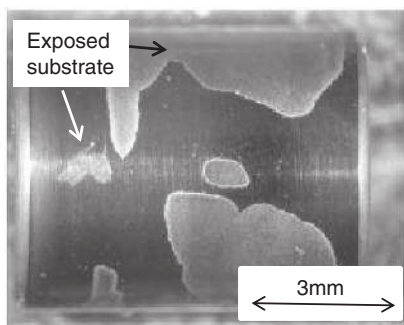


Figure 8.29 Advanced state of tearing and delamination of a non-hydrogenated, DLC-coated 100Cr6 roller after testing in formulated oil.

interfacial crack growth was obtained by preparing FIB sections adjacent to major coating tears (**Fig. 8.28**). Once the blisters were decapitated, some of them acted as sources for further interfacial crack growth – but only in the direction of rolling/sliding contact; this resulted in an appearance resembling that of a partly peeled orange (**Fig. 8.29**). The complete sequence of events from blistering through to delamination (peeling) is depicted schematically in **Fig. 8.30**. Blister formation for DLC coating materials applied to steels has been observed to take place following high-cycle dry rolling contact tests by Podgornik and Vizintin (2002) and in high-frequency ball impact testing by Ledrappier et al (2008). In both cases, blistering took place as a result of fatigue fracture growth along the DLC coating/substrate interface and the subsequent relaxation of internal coating stress.

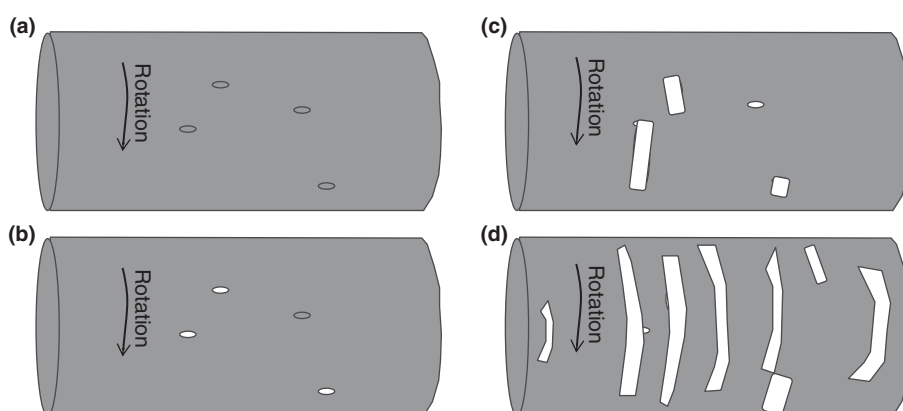


Figure 8.30 Schematic depiction of the progression of micro-delamination and tearing of ta-C DLC coating on a 100Cr6 roller bearing substrate: (a) initial blister distribution – grey-filled ellipses; (b) sheared blisters and micro-pits (substrate exposure) – white-filled ellipses; (c) initial tearing of DLC coating in direction of rolling; (d) pronounced tearing and coating loss.

### Rolling Contact Fatigue (RCF) Pitting

In the thrust bearing tests of Dearnley, Elwafi, Chittenden and Barton (2014), RCF pitting of the uncoated 100Cr6 steel began to take place after very long test durations (>500 million stress cycles). This phenomenon is well known to obey a Wöhler-type S-N-curve relationship (Kiessling, 1980) and, apart from through-hardened steel bearings, afflicts surface carburised and nitrided low-alloy steels (see **Chapter 6, Section 6.5**). Here, sub-surface cracks are initiated that initially grow away from and then, after only a few tens of micrometres' penetration, return to the surface (Savaskan & Laufer, 1984). This culminates in the ejection of a particle that leaves behind a surface pit or micro-pit with a characteristic hemispherical shape of the type shown in **Figs. 8.31** and **6.30** (also see Erdemir, 1992). Such features often exceed 200µm along their major axis. This was the main life-limiting effect for *uncoated* martensitic 100Cr6 test rollers; it was only occasionally observed in Cr<sub>2</sub>N (**Fig. 8.32**) and W-doped DLC-coated 100Cr6 (**Table 8.5**).

### Pinholing

A completely different type of pitting, herein designated 'pinholing' was also observed (**Fig. 8.33**; Yonekura et al, 2005; Dearnley et al, 2014). Such pits were much smaller (typically <5µm across) than RCF pits and were distributed uniformly over the coated surfaces. This effect was most often observed on wear-tested DLC coatings and more frequently when tests were carried out in formulated oils. Pitting phenomena reported for chill cast iron cam surfaces (Eyre & Crawley, 1980) were attributed to a negative action by ZDDP oil additives; these may have similarly promoted micro-pitting of the DLCs considered here (**Fig. 8.33**). FIB sections made through pinholes formed in DLC coatings show they often do not penetrate to the substrate; neither are they associated with any cracking (**Fig. 8.34**). Clearly, deeper

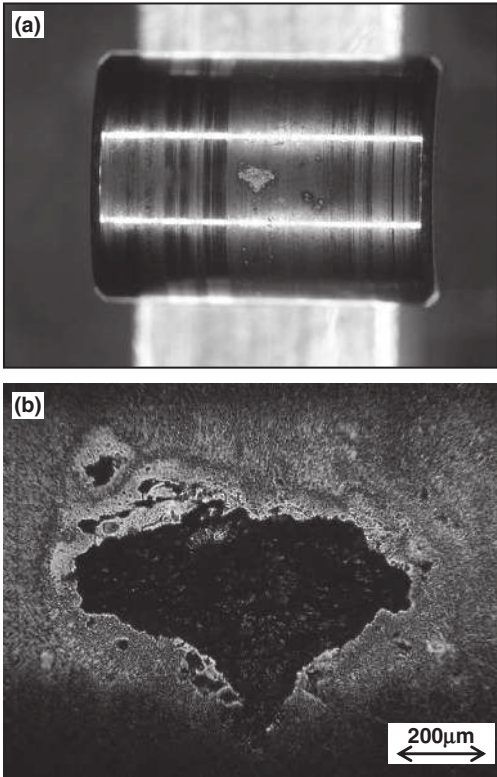


Figure 8.31 Example of a large rolling contact fatigue (RCF) pit produced in the surface of an uncoated 100Cr6 steel roller after testing in formulated (SAE 10W-40) for  $670 \times 10^6$  cycles at a maximum Hertz contact pressure of 1.5GPa: (a) low-magnification image; (b) higher-magnification image, SEM.

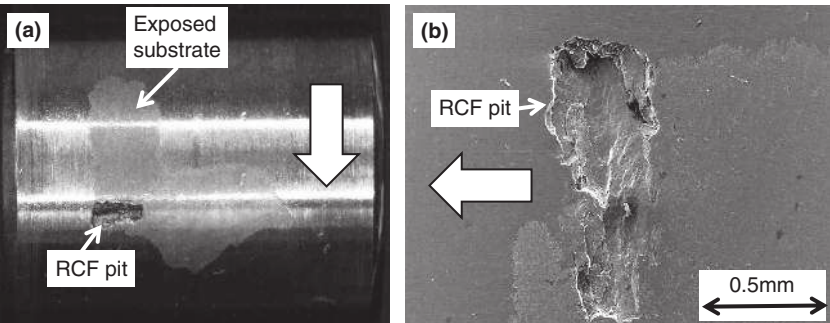


Figure 8.32  $\text{Cr}_2\text{N}$ -coated 100Cr6 test roller after 13.9 hours' testing in formulated oil (SAE 10W-40), showing: (a) delamination and RCF pit; (b) a higher-magnification view of the RCF pit (SEM). Large arrows indicate direction of rolling/sliding of roller bearing.

work is needed to uncover the fundamentals governing their formation. Fortunately, pinholes do not appear to limit the life of DLC coatings.

8.3.4 Life Limits of PVD-Coated Martensitic Steels

In the laboratory test results discussed here (Dearnley et al and Yonekura et al), only a few of the mechanisms highlighted in **Section 8.3.3** were responsible for limiting life

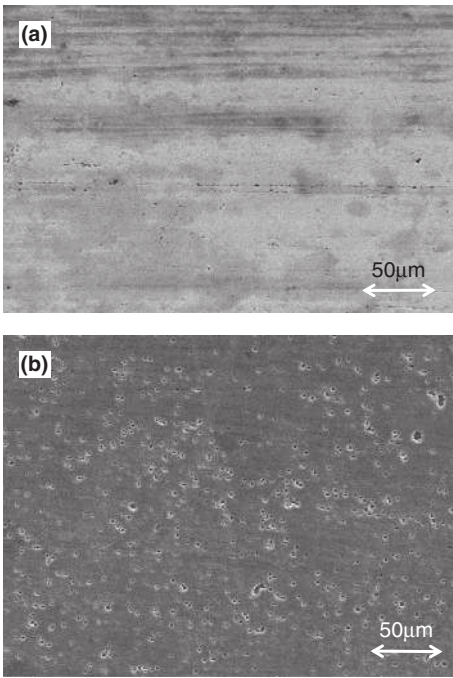


Figure 8.33 Example of pinholing on the surface of a W-doped H:DLC-coated 100Cr6 roller after approximately  $500 \times 10^6$  stress cycles at a maximum Hertz contact pressure of 1.5GPa, after testing in: (a) base oil; (b) formulated oil. Note the smooth polished surface of the non-pitted areas, attributed to micro-abrasion.

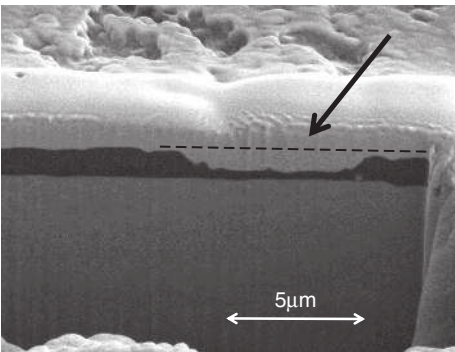


Figure 8.34 FIB section revealing the depth of a ‘pinhole’ in a non-hydrogenated, non-doped, DLC-coated 100Cr6 after several million test cycles in formulated oil. The pit (arrowed – beneath dashed line) has not reached the coating/substrate interface. (The outermost white layer is Pt applied immediately prior to ion beam sectioning to assure edge integrity.)

of uncoated and coated martensitic 100Cr6. These are summarised in **Table 8.5**. In the earliest of this work (Yonekura et al, 2005), lifetime data for uncoated, W-doped H:DLC and Cr<sub>2</sub>N coated 100Cr6 were determined (**Fig. 8.35**). (Non-doped, non-hydrogenated ta-C DLC-coated 100Cr6 was *not* investigated.) The testing indicated that PVD-Cr<sub>2</sub>N coated 100Cr6 failed prematurely via delamination after relatively short test durations (**Fig. 8.35**). In two of the tests, the delamination of the PVD-Cr<sub>2</sub>N coating triggered the formation of large RCF pits in the substrate (**Fig. 8.32**). In later research (Dearnley et al, 2014), both RCF pitting (of uncoated rollers) and delamination of ta-C DLC-coated steel (100Cr6) were observed to be statistical in character, enabling life data to be plotted on S-N graphs (number of stress cycles versus time to failure) in the manner of Wöhler diagrams

Table 8.5 Lifetime limiting wear mechanisms. Reported by Yonekura et al (2005) and Dearnley et al (2014).

Test material	Wear mechanisms observed	Mechanism(s) responsible for controlling lifetime limit
Uncoated martensitic 100Cr6	Micro-abrasion RCF pitting	RCF pitting (most cases) Few cases where life limit not reached
W-doped H:DLC-coated 100Cr6	Micro-abrasion Pinholing	Micro-abrasion (most cases) RCF pitting (2 cases only)
Non-doped, non-hydrogenated DLC-coated 100Cr6	Micro-abrasion Pinholing Delamination	Delamination (all cases)
Cr <sub>2</sub> N-coated 100Cr6	Micro-abrasion Delamination RCF pitting	Delamination (most cases) RCF pitting (2 cases only)

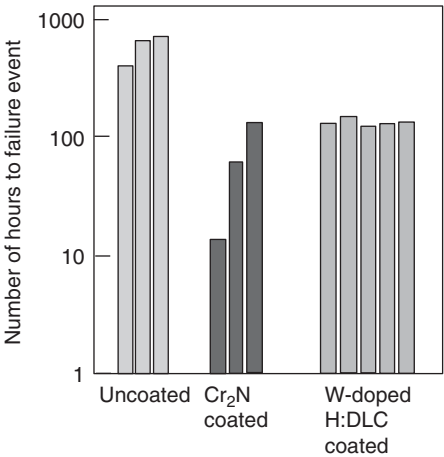


Figure 8.35 Durability of uncoated 100Cr6 compared to the same material coated with Cr<sub>2</sub>N and W-doped H:DLC. Tests conducted in a formulated SAE 10W-40 mineral oil. After Yonekura et al, 2005.

(Hertzberg, 1976). Results obtained in base oil and formulated oil are shown in **Figs. 8.36 and 8.37**, respectively. (Further testing on Cr<sub>2</sub>N coated 100Cr6 was not deemed sensible due to its poor response in previous tests – **Fig. 8.35**.) For comparison, test results of W doped H:DLC coated 100Cr6 test rollers are included in the Wöhler plots shown in (**Figs. 8.36 & 8.37**); it should be noted, however, that failures of these materials were usually governed by micro-abrasion wear of the coating. The latter data was obtained under the highest available, maximum Hertzian contact stress of 1.5GPa. Testing at lower contact pressure was not feasible for these materials, since this was very likely to have taken many weeks to complete.

DLC coatings comprise a mix of carbon that is bonded in an analogous manner to diamond (tetrahedral bonding) and graphite (Robertson, 2002). As the ratio of the diamond (Sp<sub>3</sub>) to graphitic (Sp<sub>2</sub>) bonding increases, the compressive internal stress

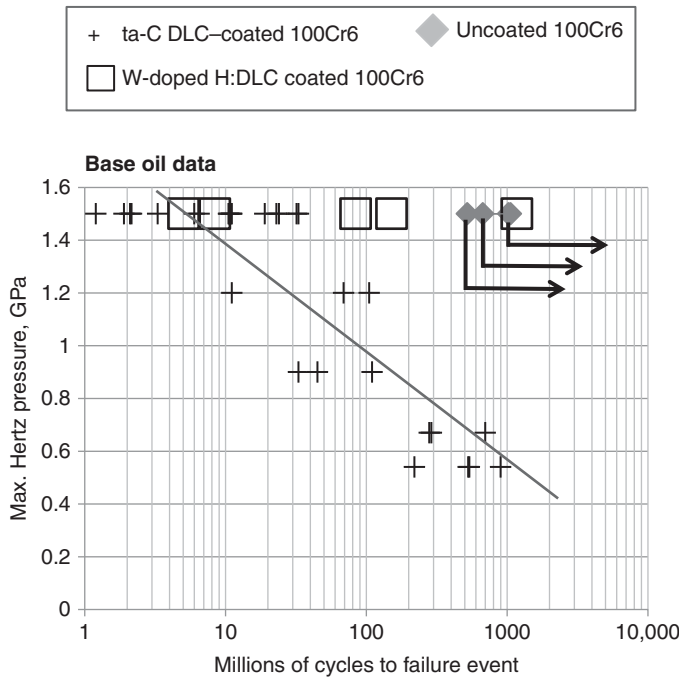


Figure 8.36 Collated S-N data for coated and uncoated 100Cr6 rollers tested against uncoated 100Cr6 bearing rings in a mineral-base oil. The line shows the linear regression fits for the ta-C-coated roller data set. Right-angled arrows indicate non-failures of uncoated rollers tested at 1.5GPa.

and its hardness proportionately increase. This is confirmed by the data shown in **Table 8.4**. The bearing test results (**Figs. 8.36 & 8.37**) clearly indicate that under mineral oil-lubricated sliding/rolling contact conditions, a high coating hardness alone is insufficient to enable high durability; the ta-C DLC coating was ~1.5 times harder than the W-doped H:DLC (**Table 8.4**), yet it failed quickly. This was attributed to the ta-C coating having a higher internal stress level than did the W-doped H:DLC. According to Peng and Clyne (1998a, b), coating delamination is promoted by a high value of internal stress; i.e., stored elastic energy in the coating drives crack growth along the coating/substrate interface, provided this exceeds the fracture strength of the interface. The W-doped H:DLC coated 100Cr6 did not suffer this mechanism and outlasted the ta-C DLC-coated variants (**Figs. 8.36 & 8.37**). Presumably, this happened because the compressive internal stress (~0.8GPa) contained in the W-doped H:DLC coatings was insufficient to cause interfacial crack initiation and growth. In contrast, the higher stored elastic energy (internal stress) within the ta-C DLC-coated variants (~5GPa) enabled relatively easy fatigue fracture along the coating/substrate interface to take place after only (in some cases) 1 to 10 million stress cycles. The main drawback of the W-doped H:DLC coatings was that they were eventually worn through via MAW. Clearly, it would be advantageous to develop these further to obtain better MAW resistance whilst maintaining a similar or lower level of internal stress. So far, this has not been achieved. Mabuchi et al (2013) have recently tested

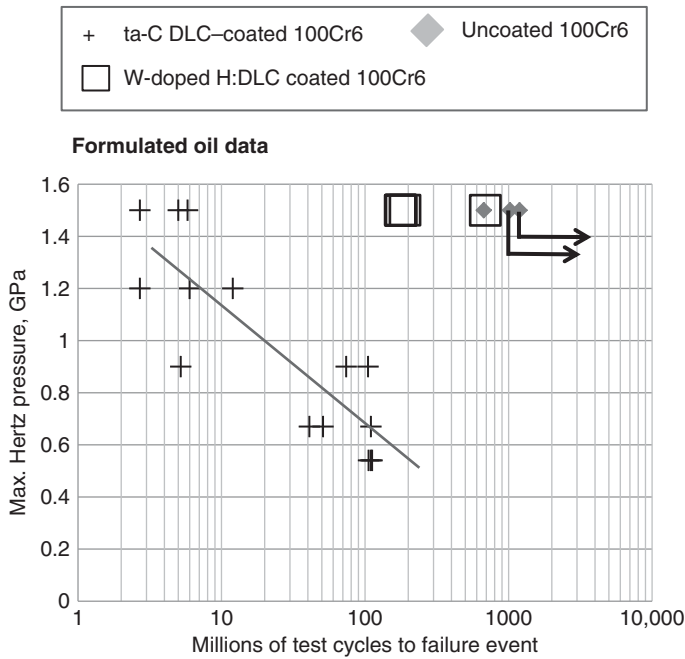


Figure 8.37 Collated S-N data for coated and uncoated 100Cr6 rollers tested against uncoated 100Cr6 bearing ring in a formulated SAE 10W-40 oil. The line shows a linear regression fit for the ta-C DLC-coated roller data set. Right-angled arrows indicate non-failures of uncoated rollers tested at 1.5GPa.

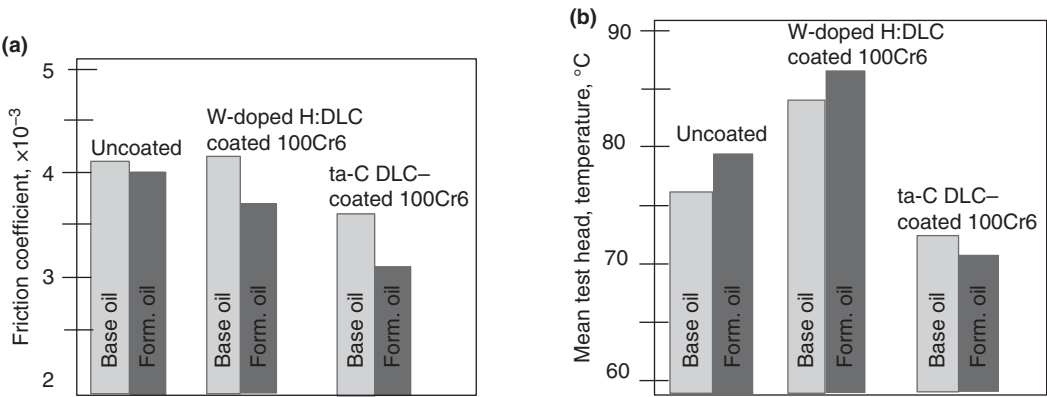


Figure 8.38 Mean (a) dynamic friction coefficients and (b) test head temperatures for uncoated and DLC-coated 100Cr6 rollers tested against uncoated 100Cr6 bearing rings in base and formulated SAE 10W-40 oil.  $P_{\max}$  was 1.5GPa in all cases. Measurements for uncoated and W-doped H:DLC coated 100Cr6 rollers were determined over the first 50 hours of testing, whilst those for ta-C DLC-coated rollers were determined over the first 2 to 6 hours, after which most tests were stopped due to coating delamination.

hydrogen-free ta-C DLC-coated steels for valve lifter applications in one series of Nissan internal combustion engines. Interestingly, they used a much lower Hertzian contact pressure ( $\sim 0.24$  GPa) than is usual for this application. This suggests that these particular devices have been redesigned to operate at contact pressures lower than those hitherto used for cam/cam-follower applications, presumably to prevent coating delamination of the type shown in **Figs. 8.29 and 8.30**.

It is often claimed that DLC coatings, per se, offer some kind of natural low-friction quality. Some of the friction measurements of the rolling/sliding contact tests considered in this section are shown in **Fig. 8.38a**; these show *insignificant differences* in the coefficients of friction between the uncoated and DLC coated 100Cr6 steel variants. Moreover, mean oil temperatures were similar for all tests (**Fig. 8.38b**). Accordingly, the observed differences in wear behaviour (under rolling/sliding contact conditions – **Figs. 8.36 and 8.37**) mainly reflect differences in the physical properties of the coated and uncoated systems concerned and were not directly influenced by the observed friction coefficients. Chemistry differences, which may have affected responses to pinholing (**Fig. 8.33**), did not influence coating life.

## References

- AE Goetze (1995), *Piston Ring Manual*, AE Goetze GMBH, Burscheid, Germany.
- Alnaqi, A. A., Shrestha, S., Barton, D. C. and Brooks, P. C. (2014), 'Optimisation of alumina coated lightweight brake rotor', Conference paper, SAE 32nd Annual Brake Colloquium and Exhibition – BRAKE 2014, Burlingame, USA, 5 October.
- Austin, L., Liskiewicz, T., Neville, A. and Tietema, R. (2012), 'The impact of the lubricant additive package on the tribological performance of diamond-like carbon coatings in simulated cam-follower conditions', Society of Vacuum Coaters, 55th Annual Technical Conference (proceedings), 28 April–3 May, 593–597.
- Barnes, A. M., Bartlem, K. and Thibon, V. R. A. (2001), 'A review of dialkylthiophosphates (ZDDPS): Characterization and role in lubricating oil', *Tribology International* **34**, 389–395.
- Barton, D. C. (2004), 'Modelling of materials for automotive braking', *International Materials Reviews* **49** (6), 379–385.
- Bec, S., Tonck, A., Georges, J. M., Coy, R. C., Bell, J. C. and Roper, G. W. (1999), 'Relationship between mechanical properties and structures of zinc dithiophosphate anti-wear films', *Proceedings of the Royal Society London A* **455**, 4181–4203.
- Becker, E. P. (2004), 'Trends in tribological materials and engine technology', *Tribology International* **37**, 569–575.
- Birch, S. (2009), 'Material opportunities (automobile engine materials)', *Automotive Engineering International* **117** (2), 22–24.
- Buran, U. (1997), 'Chromium-ceramic combination coatings for piston rings', in *Automotive Materials Technology, Autotech '97 – I MECH E Seminar Publication*, Mechanical Engineering Publications Ltd, Bury St Edmunds and London, 91–98.
- Buran, U., Christian-Mader, H., Morsbach, M. and Newman, B. A. (1986), 'Plasma sprayed coatings for piston rings – State of development and application potential', in *Surface modifications and coatings*, ASM International, Materials Park, Ohio, 255–264, edited by R. D. Sisson Jr.
- Cann, P. and Cameron, A. (1984), 'Studies of thick boundary lubrication – Influence of ZDDP and oxidized hexadecane', *Tribology International* **17** (4), 205–208.

- Dahm K. L., Black A. J., Shrestha S. and Dearnley P. A. (2009), 'Plasma electrolytic oxidation treatment of aluminium alloys for lightweight disc brake rotors', in *Braking 2009*, Proceedings of a conference held in York, UK, 9–10 June 2009, Institution of Mechanical Engineers, 53–60.
- Dahm, K. L. and Dearnley, P. A. (2000), 'On the nature, properties and wear response of S-phase (nitrogen alloyed stainless steel) coatings on AISI 316L', *Proc IMechE Part L* **214**, 181–198.
- Dearnley, P. A. (2005), 'Improving competitiveness and conserving the environment through high durability nanocomposite coatings', Final Technical Report, EC Contract G5RD-CT 2000-00430.
- Dearnley, P. A. and Aldrich-Smith, G. (2004), 'Corrosion-wear mechanisms of hard coated 316L stainless steels' *Wear* **256**, 491–499.
- Dearnley, P. A., Elwafi, A. M., Chittenden, R. J. and Barton, D. C. (2014), 'Wear and friction of diamond like carbon coated and uncoated steel roller bearings under high contact pressure oil lubricated rolling/sliding conditions', *Trans ASME Journal of Tribology* **136** (2), 021101–1 to 021101–11.
- Dearnley, P. A., Kern, E. and Dahm, K. L. (2005), 'Wear response of crystalline nanocomposite and glassy  $\text{Al}_2\text{O}_3$ -SiC coatings subjected to simulated piston ring/cylinder wall tests', *Proceedings of the Institutions of Mechanical Engineers, Part L* **219**, 121–137.
- Dearnley, P. A., Panagopoulos, K., Kern, E. and Weiss, H. (2003), 'Sliding abrasion wear assessment of  $\text{Al}_2\text{O}_3$ -SiC nano-composite coatings', *Surface Engineering* **19** (5), 373–378.
- de Barros Bouchet, M. I., Martin, J. M., Le Mogne, T. and Vacher, B. (2005), 'Boundary lubrication mechanisms of carbon coatings by MoDTC and ZDDP additives', *Tribology International* **38**, 257–264.
- Erdimir, A. (1992), 'Rolling contact fatigue and wear resistance of hard coatings on bearing steel substrates', *Surface and Coatings Technology* **54/55**, 482–489.
- European Patent EP0217126.
- Eyre, T. S. (1984), 'Wear characteristics of castings used in internal combustion engines', *Metals Technology* **11**, 81–90.
- Eyre, T. S. and Crawley, B. (1980), 'Camshaft and cam follower materials', *Tribology International* **13**, 147–152.
- Federal Mogul, on-line catalogue, accessed March 2015, <http://www.federalmogul.com/en-GB/OE/Products> (Burscheid, Germany).
- Ford Motor Company (1993a), 'Powertrain component with amorphous hydrogenated carbon film', US Patent 5,237,967, 24 August.
- Ford Motor Company (1993b), 'Powertrain component with adherent film having a graded composition', US Patent 5,249,554, 5 October.
- Gold, P. W. and Loos, J. (2002), 'Wear resistance of PVD-coatings in roller bearings', *Wear* **253**, 465–472.
- Griffiths, W. J. and Cantlow, F.-G. (1995), 'Piston and ring technology for medium speed diesel and gas engines', *Proceedings of T&N Technical Symposium*, Würzburg-Indianapolis, USA, May 1995, 23.1–23.13.
- Hertzberg, R. W. (1976), *Deformation and fracture mechanics of engineering materials*, John Wiley & Sons, New York, 418–428.
- Kano, M. and Tanimoto, I. (1991a), 'Wear resistance properties of ceramic rocker arm pads', *Wear* **145**, 153–165.
- Kano, M. and Tanimoto, I. (1991b), 'Wear mechanism of high wear-resistant materials for automotive valve trains', *Wear* **151**, 229–243.
- Kennedy, M., Hoppe, S. and Esser, J. (2012), 'Piston ring coating reduces gasoline engine friction', *MTZ Worldwide* **73** (5), 40–43.
- Kennedy, M., Hoppe, S. and Esser, J. (2014), 'Lower friction losses with new piston ring coating', *MTZ Worldwide* **75** (4), 24–28.

- Kiessling, L. (1980), 'Rolling contact fatigue of carburized and carbonitrided steels', *Heat Treatment of Metals* **7** (4), 97–101.
- Kobe Steel and Teikoku Piston Ring Company Ltd (1995), 'Hard coating material, sliding member coated with hard coating material and method for manufacturing sliding member', Japanese Patent Application JPH0727228A, 27/1/1995.
- Lampe, T., Eisenberg, S., Rodriguez, C. (2003), 'Plasma surface engineering in the automotive industry – Trends and future prospective', *Surface and Coatings Technology* **174–175**, 1–7.
- Landa, J., Illarramendi, I., Kelling, N., Woydt, M., Skopp, A. and Hartlet, M. (2005), 'Potential of thermal sprayed  $Ti_nO_{2n-1}$  coatings for substituting molybdenum based ring coatings', *Proc. 46. Jahrestagung Gesellschaft für Tribologie*, 26–28 September, Göttingen; ISBN 3-00-017102-9.
- Ledrappier, F., Langdale, C., Gachon, Y. and Vannes, B. (2008), 'Blistering and spalling of thin hard coatings submitted to repeated impacts', *Surface and Coatings Technology* **202**, 1789–1796.
- Mabuchi, Y., Higuchi, Y., Inagaki, Y., Kousaka, H. and Umehara, N. (2013), 'Wear analysis of hydrogen free diamond-like-carbon coatings under a lubricated condition', *Wear* **289–299**, 48–56.
- Mills, T. N. and Cameron, A. (1982), 'Basic studies on boundary, EP and piston-ring lubrication using a special apparatus', *ASLE Transactions* **25** (1), 117–124.
- Nicholls, J. R. (1994), 'Corrosion and wear resistance of some novel and current diesel exhaust valve materials', *Materials at High Temperatures* **12** (1), 35–46.
- Papadopoulos, P., Priest, M. and Rainforth, W. M. (2007), 'Investigation of fundamental wear mechanisms at the piston ring and cylinder wall interface in internal combustion engines', *Proceedings of the Institutions of Mechanical Engineers, Part J* **221**, 333–343.
- Peng, X. L. and Clyne, T. W. (1998a), 'Residual stress and debonding of DLC films on metallic substrates', *Diamond and Related Materials* (Switzerland) **7** (7), 944–950.
- Peng, X. L. and Clyne, T. W. (1998b), 'Mechanical stability of DLC films on metallic substrates. Part II Interfacial toughness, debonding and blistering', *Thin Solid Films* **312**, 219–227.
- Podgornik, B. and Vizintin, J. (2002), 'Rolling contact properties of ta-C coated low alloy steel', *Surface and Coatings Technology* **157**, 257–261.
- Robertson, J. (2002), 'Diamond-like amorphous carbon', *Materials Science and Engineering Reports* **37**, 129–291.
- Savaskan, T. and Laufer, E. E. (1984), 'Wear in a high speed roller bearing', *Metals Technology* **11**, 530–534.
- Scheibe, H.-J. and Schultrich, B. (1994), 'DLC film deposition by laser-arc and study of properties', *Thin Solid Films* **246**, 92–102.
- Sjöström, H. and Wikström, V. (2001), 'Diamond-like carbon coatings in rolling contacts', *Proceedings of the Institutions of Mechanical Engineers, Part J* **215**, 545–561.
- Spikes, H. (2004), 'The history and mechanisms of ZDDP', *Tribology Letters* **17** (3), 469–489.
- Stachowiak, G. W., Batchelor, A. W. and Stachowiak, G. B. (2004), *Experimental methods in tribology*, Elsevier, Amsterdam, 27–30.
- Stoney, G. G. (1909), 'The tension of metallic films deposited by electrolysis', *Proceedings of the Royal Society London A* **82**, 172–175.
- Taylor, C. M. (1991), 'Valve train lubrication analysis', *Proceedings of the 17th Leeds-Lyon Symposium in Tribology*, 4–7 September, 1990, Elsevier, 119–131.
- Vingsbo, O., Hogmark, S., Jönsson, B. and Ingemarsson, A. (1986), 'Indentation hardness of surface coated materials', in *Microindentation techniques in materials science and engineering*, ASTM Special Technical Publication 889, American Society for Testing and Materials, Ann Arbor, USA, 257–271, edited by P. Blau and B. Lawn.
- Yonekura, D., Chittenden, R. J. and Dearnley, P. A. (2005), 'Wear mechanisms of steel roller bearings protected by thin, hard and low friction coatings', *Wear* **259**, 779–788.